Autophagy-independent functions of UVRAG are essential for peripheral naive T-cell homeostasis

Samia Afzal[a,b,1], Zhenyue Hao[b,1], Momoe Itsumi[b,c], Yasser Abouelkheer[b], Dirk Brenner[b,d], Yunfei Gao[b], Andrew Wakeham[b], Claire Hong[b], Wanda Y. Li[b], Jennifer Sylvester[b], Syed O. Gilani[b], Anne Brüstle[b,e], Jillian Haight[b], Annick J. You-Ten[b], Gloria H. Y. Lin[b], Satoshi Inoue[b], and Tak W. Mak[a,b,2]

[a]Department of Immunology, University of Toronto, Toronto, Ontario, Canada M5S 1A8; [b]Campbell Family Cancer Research Institute, University Health Network, Toronto, Ontario, Canada M5G 2C1; [c]Department of Urology, Kyushu University, 3-1-1 Maidashi, Higashi-ku, Fukuoka. 812-8582, Japan; [d]Department of Infection and Immunity, Luxembourg Institute of Health, 84, Val Fleuri, L-1526, Luxembourg; and [e]Pathogens and Immunity Department, Australian National University, Acton Act 2601, Canberra, Australia

Contributed by Tak W. Mak, December 15, 2014 (sent for review November 13, 2014; reviewed by Douglas R. Green)

UV radiation resistance-associated gene (UVRAG) encodes a tumor suppressor with putative roles in autophagy, endocytic trafficking, and DNA damage repair but its in vivo role in T cells is unknown. Because conditional homozygous deletion of *Uvrag* in mice results in early embryonic lethality, we generated T-cell–specific UVRAG-deficient mice that lacked UVRAG expression specifically in T cells. This loss of UVRAG led to defects in peripheral homeostasis that could not be explained by the increased sensitivity to cell death and impaired proliferation observed for other autophagy-related gene knockout mice. Instead, UVRAG-deficient T-cells exhibited normal mitochondrial clearance and activation-induced autophagy, suggesting that UVRAG has an autophagy-independent role that is critical for peripheral naive T-cell homeostatic proliferation. In vivo, T-cell–specific loss of UVRAG dampened $CD8^+$ T-cell responses to LCMV infection in mice, delayed viral clearance, and impaired memory T-cell generation. Our data provide novel insights into the control of autophagy in T cells and identify UVRAG as a new regulator of naïve peripheral T-cell homeostasis.

T-cell homeostasis | UVRAG-deficient mice | autophagy | embryonic lethality

Genes encoding elements of the autophagy machinery are expressed in T lymphocytes, and autophagy occurs in both resting and activated T cells (1, 2). Studies of knockout mice bearing T-cell–specific deletions of autophagy genes, including ATG3, ATG5, ATG7 and Beclin-1, have revealed an indispensable role for autophagy in T-cell homeostasis (1, 3–5), but have also raised important questions about regulation of this process in these cells.

UV radiation resistance-associated gene (UVRAG) was initially identified as a molecule that rescues the UV sensitivity of Xeroderma Pigmentosum group C cells (6), but has since attracted attention for its dual roles in mammalian cell autophagy. UVRAG promotes autophagosome formation in vitro by associating with Beclin-1 and up-regulating class III phosphatidylinositol 3-kinase activity (7–9). Subsequently, UVRAG promotes autophagosome maturation by binding to the C/Vps HOPS complex (10, 11). Accordingly, autophagy is defective in fibroblasts and cardiomyocytes of mice bearing transposon-induced *Uvrag* deletion (12). In cancer cells, UVRAG overexpression enhances autophagy and reduces proliferation, suggesting that UVRAG may control cell growth by regulating autophagy (8, 9). However, several lines of evidence indicate that UVRAG has autophagy-independent functions, at least in vitro: (*i*) UVRAG promotes endocytic trafficking in endosomes by interacting with the C/Vps complex (7). (*ii*) In *Drosophila*, UVRAG mediates proper organ rotation through regulation of Notch receptor endocytosis (13). (*iii*) UVRAG maintains chromosomal stability by mediating DNA damage repair (14); and (*iv*) UVRAG suppresses apoptosis by regulating Bax localization (15). Therefore, the function of UVRAG in any given context is best studied in vivo. Because T cells offer a physiologically relevant and easily manipulated system for studying gene function and regulation, we generated and characterized conditional UVRAG-deficient Lck-Cre mice and examined UVRAG functions in T-cell biology in vivo.

Results

UVRAG Is Essential for Murine Embryogenesis but Dispensable for Thymocyte Development. We used the Cre-loxP system to create conditional UVRAG knockout mice ($UR^{fl/fl}$ mice, Fig. S1*A*). When complete loss of UVRAG was induced by crossing these mutants to Deleter-Cre mice, embryonic lethality resulted by day E7.5. To circumvent this lethality, $UR^{fl/fl}$ mice were bred with Lck-Cre transgenic mice to delete UVRAG specifically in T cells ($UR^{fl/fl}$;*Lck-Cre* mice). These mutants were born at the expected Mendelian ratio and appeared phenotypically normal. High efficiency of UVRAG deletion in their peripheral T cells was confirmed by immunoblotting (Fig. S1*B*).

We first subjected $UR^{fl/fl}$;*Lck-Cre* and control $UR^{fl/fl}$ littermates to comprehensive analyses of T-cell production in the thymus. Early thymocyte development through the double negative 1 (DN1) to DN4 stages, as measured by CD25 and CD44 expression, was intact in the absence of UVRAG (Fig. S1*C*). Although single positive (SP) $CD4^+$ and $CD8^+$ thymocytes appeared to be modestly reduced in $UR^{fl/fl}$;*Lck-Cre* mice compared with controls (Fig. 1*A*), this difference was not statistically

Significance

T-cell homeostasis is a tightly regulated process that ensures a constant number of naïve T cells in the periphery of an organism. Mechanisms that promote the survival and homeostatic proliferation of naïve peripheral T cells are essential for maintaining this balance and thus effective immunity against pathogens and incipient tumors. We have identified UV radiation resistance-associated gene (UVRAG), an autophagic tumor suppressor in many cell lineages, as a novel nonautophagic regulator of naïve peripheral T cell homeostasis. Furthermore, our findings distinguish UVRAG from other autophagy-related genes and indicate that this regulator may have important nonautophagic functions that are cell type-specific.

Author contributions: S.A., Z.H., and T.W.M. designed research; S.A., M.I., Y.A., D.B., Y.G., A.W., C.H., W.Y.L., J.S., S.O.G., A.B., and A.J.Y.-T. performed research; M.I., J.H., G.H.Y.L., and S.I. contributed new reagents/analytic tools; S.A., M.I., Y.A., D.B., Y.G., and A.B. analyzed data; S.A. and T.W.M. wrote the paper; and Z.H. generated the UVRAG conditional knockout mouse with the help of A.W., C.H., W.Y.L., J.S., and A.J.Y.-T.

Reviewers included: D.R.G., St. Jude Children's Research Hospital.

The authors declare no conflict of interest.

Freely available online through the PNAS open access option.

[1]S.A and Z.H. contributed equally to this work.

[2]To whom correspondence should be addressed. Email: tmak@uhnres.utoronto.ca.

This article contains supporting information online at www.pnas.org/lookup/suppl/doi:10.1073/pnas.1423588112/-/DCSupplemental.

significant. Similarly, expression levels of TCRβ, CD44, CD62L, and CD25 were equivalent on $UR^{fl/fl}$;*Lck-Cre* and control thymocytes (Fig. S1*D*). Thus, UVRAG is dispensable for thymocyte development and maturation.

$UR^{fl/fl}$;Lck-Cre Mice Exhibit Peripheral T-Cell Lymphopenia. We next compared secondary lymphoid organs of $UR^{fl/fl}$;*Lck-Cre* and $UR^{fl/fl}$ littermates and found significant decreases in cellularity in mutant spleen and lymph nodes (LN) (Fig. S2*A*). $UR^{fl/fl}$;*Lck-Cre* spleen, LN and peripheral blood (PBL) all showed marked reductions in proportions of $CD4^+$ and $CD8^+$ peripheral T cells (Fig. 1B, left and Fig. S2*B*). Furthermore, in mutant spleen, the total $CD4^+$ T-cell number (4.69×10^6 cells) was <50% of controls (10.9×10^6 cells; $P < 0.0003$), a difference even more pronounced for $CD8^+$ T cells ($UR^{fl/fl}$, 5.83×10^6 vs. $UR^{fl/fl}$;*Lck-Cre*, 1.76×10^6; $P < 0.00007$) (Fig. 1B, right). A similar imbalance in $CD4^+$ and $CD8^+$ T-cell numbers occurred in mutant LN (Fig. 1B). This general reduction in peripheral $CD4^+$ and $CD8^+$ T cells was maintained in aged $UR^{fl/fl}$;*Lck-Cre* mice (Fig. S2*C*), indicating that the deficit was not restricted to the initial maturation of the immune system in young mice. Interestingly, loss of UVRAG did not affect the homeostasis of $CD4^+CD25^+$ $Foxp3^+$ regulatory T cells (Tregs) in any lymphoid tissue (Fig. S2*D*). Thus, UVRAG influences the homeostasis of conventional peripheral T cells.

UVRAG Deletion Enhances Memory T-Cell Marker Expression and Promotes Hyperproliferation. In lymphopenic mice, any residual peripheral T cells present usually express a marker profile characteristic of either activated effector T cells or central memory T cells (16, 17). Activated effector T cells and effector memory T cells express $CD62L^{lo}CD44^{hi}$, whereas central memory T cells are $CD62L^{hi}CD44^{hi}$ and naïve T cells are $CD62L^{hi}$ $CD44^{lo}$. We found that a greater proportion of $CD8^+$ T cells in the spleen and LN of $UR^{fl/fl}$;*Lck-Cre* mice were $CD62L^{hi}CD44^{hi}$ in profile compared with $UR^{fl/fl}$ T cells (Fig. 2*A* and Fig. S3 *A* and *B*), implying that a loss of UVRAG causes a reduction in naïve T cells but preferential retention of central memory T cells. Interestingly, the observed up-regulation of CD44 on the latter cells was not accompanied by an increase in CD25 or CD69, indicating that these UVRAG-deficient T cells were not activated (Fig. 2*B* and Fig. S3*C*). These findings support our hypothesis that UVRAG regulates peripheral T-cell homeostatic proliferation.

ATG5-, ATG7-, or Beclin-1–deficient mice at steady-state all exhibit lymphopenia due to increased apoptosis and impaired proliferation of peripheral T cells (1, 3–5). However, we found no differences in apoptosis in cultures of T cells isolated from spleen or LN of steady-state $UR^{fl/fl}$ and $UR^{fl/fl}$;*Lck-Cre* littermates (Fig. 2*C*). We then stimulated $UR^{fl/fl}$ and $UR^{fl/fl}$;*Lck-Cre* thymocytes and splenic T cells in vitro with a panel of apoptotic stimuli that included anti-CD3 antibody (Ab), γ-irradiation (IR), UV irradiation, and anti-Fas Ab. Surprisingly, no significant differences in apoptotic sensitivity were detected between $UR^{fl/fl}$ and $UR^{fl/fl}$;*Lck-Cre* T cells (Fig. S4 *A* and *B*). Thus, the reduced T-cell numbers in $UR^{fl/fl}$;*Lck-Cre* mice are not due to increased apoptosis.

In addition to enhanced apoptosis, ATG3-, ATG5-, ATG-7, and Beclin-1–deficient T cells exhibit impaired proliferation in response to T-cell receptor (TCR) engagement (1, 3–5). To test the role of UVRAG in TCR signaling, we stimulated naïve $UR^{fl/fl}$ and $UR^{fl/fl}$;*Lck-Cre* T cells with anti-CD3/CD28 Abs in vitro. Mutant $CD4^+$ and $CD8^+$ T cells exhibited hyperproliferation when measured by either ^{3}H-thymidine incorporation or carboxyfluorescein succinimidyl ester (CFSE) dilution, and at all anti-CD3 Ab concentrations tested (Fig. 2*D* and Fig. S4*C*). Notably, $UR^{fl/fl}$;*Lck-Cre* naive T cells generated lymphoblasts when stimulated at lower concentrations of anti-CD3 Ab than did $UR^{fl/fl}$ naive T cells, indicating that loss of UVRAG reduces the activation threshold. Thus, in contrast to other autophagy genes, UVRAG may be a negative regulator of T-cell proliferation induced by TCR engagement in vitro. These findings differentiate the UVRAG-deficient phenotype from that of other autophagy-related genes (1, 3–5), and imply an autophagy-independent role for UVRAG in T cells.

UVRAG Function in Peripheral T Lymphocytes Is Cell-Intrinsic and Required for Homeostatic Proliferation. To test whether the defect in peripheral T-cell maintenance associated with UVRAG deficiency was cell-intrinsic, we generated mixed bone marrow (BM) chimeras in Rag-$2^{-/-}$ mice (which lack both B and T cells) and compared the relative contributions of $CD45.1^+$ vs. $CD45.2^+$ donor BM cells to the reconstitution of lymphoid organs in these animals. In control chimeras, where the CD45.1 and CD45.2 donor cell populations both expressed UVRAG, the B and T cells present at 1.5 mo postreconstitution had originated equally from $CD45.1^+$ and $CD45.2^+$ donor BM cells (Fig. S5*A*). In mutant chimeras bearing UVRAG sufficient $CD45.1^+$ cells plus UVRAG deficient $CD45.2^+$ cells, the B-cell compartment showed a 1:1 ratio of $CD45.1^+$ vs. $CD45.2^+$ expression, indicating equal derivation, but T cells were overwhelmingly derived from UVRAG sufficient $CD45.1^+$ cells (ratio of 10:1 in spleen and LN, and 6:1 in PBL) (Fig. 3 *A* and *B*). Skewing toward the UVRAG sufficient donor population was even greater when the mutant chimeras were examined at 4 mo postreconstitution (Fig. 3*B*). Interestingly, UVRAG was more important for the reconstitution of $CD8^+$ T cells than $CD4^+$ T cells (Fig. 3*C*). All of these findings are consistent with the phenotype of our $UR^{fl/fl}$;*Lck-Cre* mice at steady-state, and suggest that UVRAG plays a crucial cell-autonomous role in maintaining peripheral T-cell numbers.

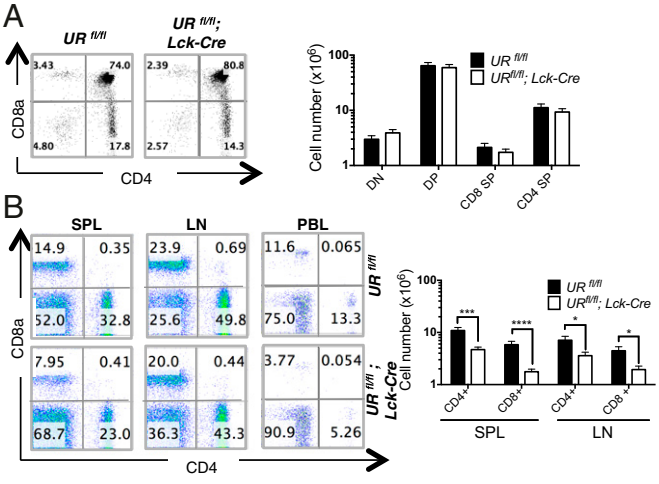

Fig. 1. Impaired T-cell homeostasis in the periphery of $UR^{fl/fl}$;*Lck-Cre* mice. (*A*) (*Left*) Flow cytometric analysis of DN, DP and SP thymocytes from $UR^{fl/fl}$ and $UR^{fl/fl}$;*Lck-Cre* mice. Numbers are percentages of total live thymocytes and are representative of four mice per group. (*Right*) Quantitation of the mean absolute numbers ± SEM of the indicated thymocyte subsets in the thymus of $UR^{fl/fl}$ and $UR^{fl/fl}$;*Lck-Cre* mice. Results are derived from 13 independent experiments involving 1–4 mice per group. (*B*) (*Left*) Flow cytometric analysis of $CD4^+$ and $CD8^+$ T cells isolated from spleen (SPL), lymph node (LN) and peripheral blood (PBL) of $UR^{fl/fl}$ and $UR^{fl/fl}$;*Lck-Cre* mice (n = 13–16 per group). Numbers are percentages of total live lymphocytes. Results are representative of 13 trials. (*Right*) Quantitation of mean absolute numbers ± SEM of $CD4^+$ and $CD8^+$ T cells in the SPL and LN of $UR^{fl/fl}$ and $UR^{fl/fl}$;*Lck-Cre* mice (n = 13–16 mice per group). *$P < 0.05$; ***$P < 0.0005$; ****$P < 0.00005$.

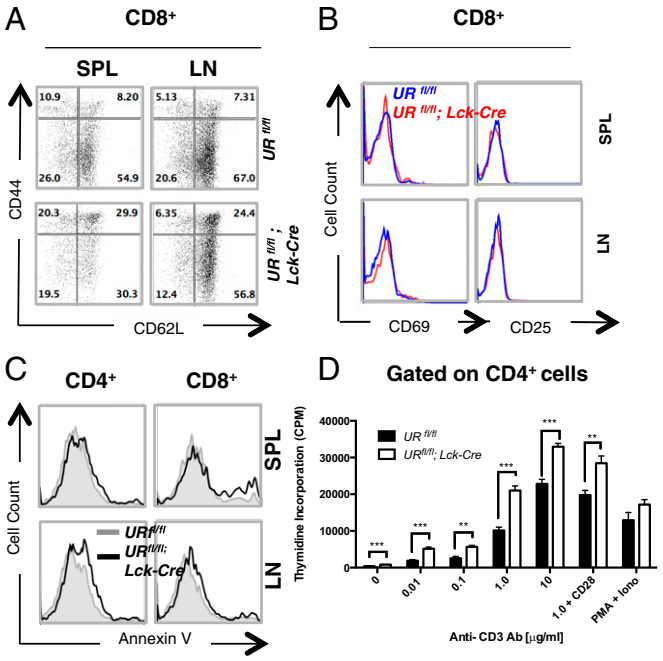

Fig. 2. In vitro characterization of marker profile, apoptosis and anti-CD3-stimulated proliferation of UVRAG-deficient T cells. (*A*) Flow cytometric analysis of CD8$^+$ T cells that were isolated from SPL and LN of littermate *UR*$^{fl/fl}$ and *UR*$^{fl/fl}$*;Lck-Cre* mice (n = 1–4 per group) and immunostained to detect CD44 and CD62L. Numbers are percentages of total CD8$^+$ T cells and are representative of eight trials. (*B*) Flow cytometric plot of CD69 and CD25 expression by the CD8$^+$ T cells in *A*. Data are representative of six independent experiments involving 1–4 mice per group. (*C*) Flow cytometric analysis of apoptosis of resting CD4$^+$ or CD8$^+$ T cells that were isolated from SPL or LN of *UR*$^{fl/fl}$ (gray line) or *UR*$^{fl/fl}$*;Lck-Cre* (black line) mice (n = 1–4 per group) and stained with Annexin V. Data are representative of three independent experiments. (*D*) ^{3}H-thymidine incorporation assay of proliferation in vitro of naïve peripheral CD4$^+$ T cells that were isolated from *UR*$^{fl/fl}$ or *UR*$^{fl/fl}$*;Lck-Cre* mice (n = 2–4 per group) and stimulated for 72 h in vitro with the indicated concentrations of plate-bound anti-CD3 Ab, or 1.0 μg/mL plate-bound anti-CD3 Ab plus 0.1 μg/mL plate-bound anti-CD28 Ab, or with PMA (10 ng/mL) plus ionomycin (Iono; 100 ng/mL). Data are the cumulative mean cpm ± SEM of triplicates from two independent experiments. $^{**}P < 0.005$; $^{***}P < 0.0005$.

To determine whether the increase in the central memory T-cell population in steady-state *UR*$^{fl/fl}$*;Lck-Cre* mice was due to the lymphopenic environment or to an impaired UVRAG function, we compared CD44 and CD62L expression by T cells in BM chimeras created by reconstituting lethally-irradiated C57BL/6 recipient (CD45.2) mice with a 1:1 mixture of *UR*$^{fl/fl}$ (CD45.1) and *UR*$^{fl/fl}$*;Lck-Cre* (CD45.2) donor cells. Indeed, the effector (CD44^{hi}CD62L^{lo}) and central memory (CD44^{hi}CD62L^{hi}) populations derived from *UR*$^{fl/fl}$*;Lck-Cre* donor cells were comparable to those derived from *UR*$^{fl/fl}$ donor cells (Fig. 3*D* and Fig. S5*B*). Thus, the increase in memory cell markers on UVRAG-deficient T cells is likely due to the lymphopenic environment and not to loss of a UVRAG function.

To test whether UVRAG is indeed essential for the homeostatic proliferation of naïve peripheral T cells, we compared the expansion of *UR*$^{fl/fl}$*;Lck-Cre* and *UR*$^{fl/fl}$ naïve T cells transplanted into a lymphopenic host. We purified naïve T cells from *UR*$^{fl/fl}$ (CD45.1) and *UR*$^{fl/fl}$*;Lck-Cre* (CD45.2) mice, labeled them separately with CFSE, and adoptively transferred a 1:1 mixture of these cells into lethally-irradiated C57BL/6 recipients (CD45.1/2). At 6 d posttransfer, T cells were recovered from recipients' spleens and LN, and cell numbers and marker profiles were assessed by flow cytometry. A bias toward *UR*$^{fl/fl}$ (CD45.1) T cells was observed in recipient spleen and LN (Fig. 3*E*). Moreover, *UR*$^{fl/fl}$*;Lck-Cre* (CD45.2) T cells showed decreased proliferation as evidenced by CFSE dilution (Fig. 3*F*). These data strongly suggest that UVRAG plays an essential cell-intrinsic role in maintaining peripheral T-cell numbers, and that the lymphopenia observed in *UR*$^{fl/fl}$*;Lck-Cre* mice is due to impaired T-cell homeostatic proliferation.

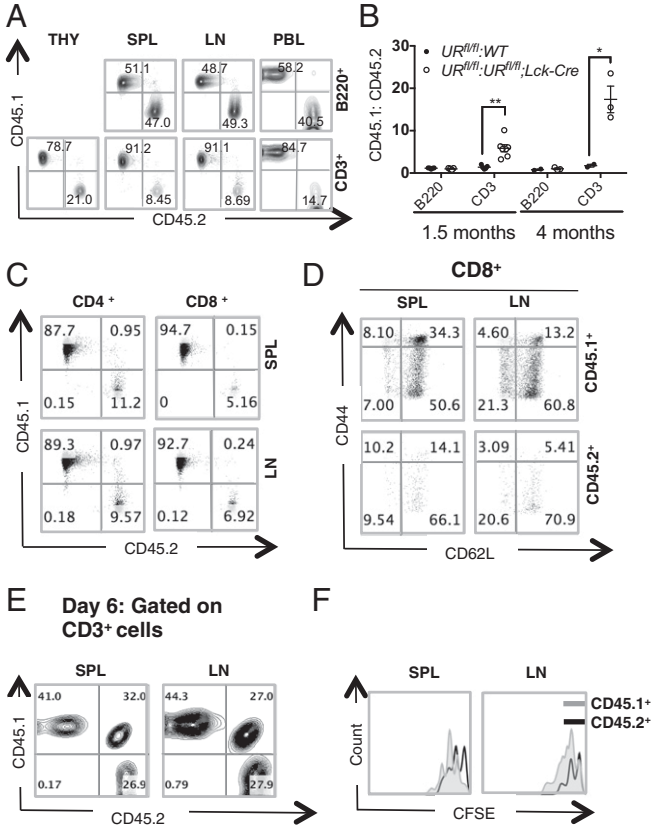

Fig. 3. UVRAG-deficient T cells show defects in bone marrow reconstitution and lymphopenia-induced homeostatic proliferation. (*A*) Flow cytometric analysis of B and T-cell populations in the indicated lymphoid tissues of mutant BM chimeras. BM cells from CD45.1$^+$ *UR*$^{fl/fl}$ and CD45.2$^+$ *UR*$^{fl/fl}$*;Lck-Cre* mice were mixed 1:1 and i.v.-injected into sublethally irradiated Rag-2$^{-/-}$ mice (n = 3–4 mice per group). In control experiments, a 1:1 mixture of BM cells from CD45.1$^+$ *UR*$^{fl/fl}$ and CD45.2$^+$ *UR*$^{fl/fl}$ mice was injected. After 1.5 mo, lymphoid tissue reconstitution was assessed by measuring the relative contributions of CD45.1$^+$ and CD45.2$^+$ BM cells to the regeneration of B (B220$^+$) and T (CD3$^+$) cell populations in thymus (THY), SPL, LN and PBL of chimeric recipients. Numbers are percentages of live B220$^+$ or CD3$^+$ cells. Results are representative of four trials. (*B*) Quantitation of ratio of CD45.1$^+$ vs. CD45.2$^+$ BM cells contributing to the reconstitution of B- and T-cell populations in PBL of the mice in *A* at 1.5 mo or 4 mo after reconstitution. Each data point represents a single mouse and horizontal bars are geometric mean values. Data are representative of four independent experiments involving 3–4 mice per group. $^{*}P < 0.05$; $^{**}P < 0.005$. (*C*) Flow cytometric analysis of reconstitution of CD4$^+$ and CD8$^+$ populations in SPL and LN of the mutant chimeras in *A*. Numbers are percentages of live CD4$^+$ and CD8$^+$ cells. Results are representative of 2 experiments involving 3–5 mice per group. (*D*) Flow cytometric analysis of CD44 and CD62L expression by live CD8$^+$ T cells from SPL and LN of the mutant chimeras (n = 3) in *A*. Results are representative of two trials. (*E*) Flow cytometric analysis of CFSE-labeled *UR*$^{fl/fl}$ (CD45.1$^+$) or *UR*$^{fl/fl}$*;Lck-Cre* (CD45.2$^+$) naïve T cells that were transferred into irradiated C57BL/6 (CD45.1/CD45.2) lymphopenic hosts and recovered from SPL and LN 6 d later. Numbers are percentages of live CD3$^+$ T cells that were CD45.1$^+$ or CD45.2$^+$. Results are representative of two trials involving 3–4 mice per group. (*F*) Flow cytometric plot of CFSE dilution in *UR*$^{fl/fl}$ (CD45.1$^+$) and *UR*$^{fl/fl}$*;Lck-Cre* (CD45.2$^+$) T cells among live CD3$^+$ cells isolated from SPL or LN of one recipient in *E*. Data are representative of two independent experiments.

UVRAG Does Not Appear to Be Required for Canonical Autophagy in T Cells. The well described role of UVRAG in autophagy in vitro prompted us to determine whether the phenotypes observed in our *UR$^{fl/fl}$;Lck-Cre* mice were due to impaired autophagy. We first examined the mitochondrial content of UVRAG-deficient peripheral T cells. Normal T cells are known to decrease their mitochondrial mass upon thymic exit (5), a finding we confirmed (Fig. 4*A*). This mitochondrial down-regulation is at least partly attributable to mitophagy (autophagic destruction of mitochondria), as T cells in mice lacking ATG3, ATG5 or ATG7 are unable to reduce their mitochondria sufficiently and undergo death caused by accumulation of reactive oxygen species (ROS) (4, 5, 18). To compare mitochondrial content in *UR$^{fl/fl}$* and *UR$^{fl/fl}$;Lck-Cre* T lineage cells, we stained thymic, splenic and LN T-cell populations with Mitotracker and measured mitochondrial mass by flow cytometry. No appreciable differences were observed (Fig. 4*B*), suggesting that UVRAG-deficient T cells can reduce their mitochondria normally upon thymic exit and that UVRAG is not required for mitophagy.

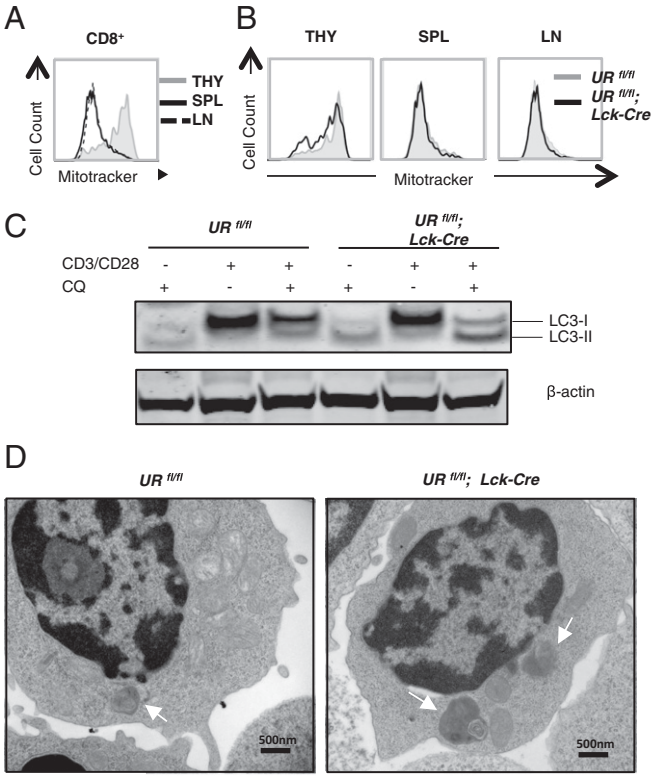

Fig. 4. Activation-induced autophagy is enhanced in UVRAG-deficient T cells. (*A*) Flow cytometric plot of mitochondrial content in CD8$^+$ SP thymocytes (THY) or peripheral CD8$^+$ T cells isolated from SPL and LN of steady-state *UR$^{fl/fl}$* mice ($n = 3$) and stained with FITC-Mitotracker. Results are representative of three trials. (*B*) Flow cytometric plot of mitochondrial content of CD8$^+$ T cells isolated from the indicated lymphoid tissues of one *UR$^{fl/fl}$* and one *UR$^{fl/fl}$;Lck-Cre* mouse. Data were obtained as in *A* and are representative of two independent experiments involving 2–3 mice per group. (*C*) Autophagic flux in T cells that were isolated from SPL and LN of *UR$^{fl/fl}$* and *UR$^{fl/fl}$;Lck-Cre* mice ($n = 2$ per group) and activated in vitro overnight with 2 μg/mL anti-CD3 plus 0.2 μg/mL anti-CD28 Abs, with or without 25 nM chloroquine (CQ). Lysates were immunoblotted to detect LC3I/II. β-actin, loading control. Results are representative of three independent experiments. (*D*) Transmission electron micrographs showing autophagosomes in naïve peripheral T cells that were isolated from SPL and LN of *UR$^{fl/fl}$* and *UR$^{fl/fl}$;Lck-Cre* mice ($n = 2$ per group) and activated in vitro with anti-CD3/CD28 Abs in the presence of CQ. Scale bars represent 500 nm and autophagosomes are highlighted with white arrowheads. Images are representative of one experiment.

To determine whether UVRAG is necessary for the prominent autophagosome formation induced upon T-cell activation (1, 19), we cultured *UR$^{fl/fl}$* and *UR$^{fl/fl}$;Lck-Cre* naïve peripheral T cells in complete medium, or in medium containing anti-CD3 plus anti-CD28 Abs, with or without the autophagy inhibitor chloroquine (CQ). Autophagy was then measured by the LC3 lipidation assay and by transmission electron microscopy. We found that anti-CD3/CD28 treatment increased LC3-I and LC3-II levels in control *UR$^{fl/fl}$* T cells (Fig. 4*C*, *Left*), consistent with published data (19). This elevation was comparable in UVRAG-deficient T cells (Fig. 4*C*, *Right*). However, whereas only a faint LC3-II band was present in CQ-treated *UR$^{fl/fl}$* T cells (as expected), large amounts of LC3-II were present in CQ-treated mutant T cells (Fig. 4*C*). Transmission electron microscopy confirmed robust autophagosome formation not only in anti-CD3/CD28-stimulated *UR$^{fl/fl}$* T cells but also in anti-CD3/CD28-stimulated *UR$^{fl/fl}$;Lck-Cre* T cells (Fig. 4*D*). Thus, in contrast to other autophagy-related genes, and to UVRAG's function in other cell types, UVRAG may be dispensable for autophagy in T cells. Collectively, our results suggest that UVRAG regulates peripheral T-cell numbers by an autophagy-independent mechanism.

UVRAG Biases Th Effector Generation Toward Th1 Cells. We consistently observed a differential effect of UVRAG loss on CD4$^+$ vs. CD8$^+$ T cells, in both *UR$^{fl/fl}$;Lck-Cre* mice at steady-state and in BM chimeras. In line with these observations, UVRAG protein was differentially expressed in CD4$^+$ and CD8$^+$ peripheral T cells (Fig. S6*A*), implying that UVRAG may play different roles in different T-cell subsets.

To study UVRAG functions specific to CD4$^+$ T cells, we investigated T helper (Th) effector cell differentiation *in vitro*. We isolated naive CD4$^+$CD62L$^+$ peripheral T cells from *UR$^{fl/fl}$* and *UR$^{fl/fl}$;Lck-Cre* mice and primed these cells in vitro with anti-CD3/CD28 Abs for 3 d in the presence of specific cytokine mixtures known to drive Th0, Th1, Treg or Th17 cell differentiation (*Methods*). After this polarization period, cytokine production was evaluated by intracellular cytokine staining and flow cytometry. Whereas the differentiation of Th0, Treg and Th17 cells was not altered in the absence of UVRAG, we observed almost twice as many Th1 cells in the mutant cultures (72%) as in control cultures (42%) (Fig. S6*B*).

To test the in vivo relevance of this bias toward Th1 differentiation, we exploited experimental autoimmune encephalomyelitis (EAE) induction, which is a mouse model of human multiple sclerosis (MS). Injection of wild type mice with myelin oligodendrocyte glycoprotein (MOG) peptide plus pertussis toxin results in the development of severe EAE within 30 d, and both Th1 and Th17 cells are required for disease pathogenesis (20–23). T-cell–specific Beclin-1–deficient mice, which are lymphopenic and exhibit defects in Th1 and Th17 differentiation, are completely resistant to EAE induction (3). Although we speculated that the increased Th1 cell differentiation we observed in our cultures of UVRAG-deficient T cells might exacerbate the frequency and severity of EAE developing in *UR$^{fl/fl}$;Lck-Cre* mice, no differences from controls in EAE onset or severity were observed (Fig. S6*C*). This result suggests that the skewing toward Th1 cells in *UR$^{fl/fl}$;Lck-Cre* mice is sufficient to compensate for the lymphopenia in these mutants and supplies enough autoreactive T cells to induce EAE.

UVRAG Is Essential for CD8$^+$ T-Cell Expansion and MPEC Generation During Acute LCMV Infection. To investigate the role of UVRAG in CD8$^+$ T-cell–driven immune responses, we used an LCMV infection model. In immunocompetent mice, infection with the Armstrong strain of LCMV results in acute disease, robust CD8$^+$ T-cell expansion, rapid clearance of the virus and the generation of long-lived memory CD8$^+$ T cells. We infected *UR$^{fl/fl}$* and *UR$^{fl/fl}$;*

Lck-Cre mice with Armstrong LCMV (10^5 pfu) and analyzed T-cell responses at 8 d postinfection (Fig. S7*A*). Antigen-specific $CD8^+$ T-cell responses to the immunodominant LCMV GP33 and NP396 epitopes were measured using fluorescently-labeled tetramers. Both $UR^{fl/fl}$ and $UR^{fl/fl}$;*Lck-Cre* mice exhibited robust proliferation of $CD8^+$ T cells following LCMV infection, but the mutants continued to show a persistent and significant reduction in $CD4^+$ and $CD8^+$ T-cell numbers compared with controls (Fig. 5*A*). Importantly, the mutants harbored a decreased number of $CD8^+$ T cells directed against GP33 (Fig. 5*B*). Consequently, these animals exhibited relatively high viral titres in the brain, lung, spleen and kidney at day 8 postinfection, in contrast to the much lower viral titres in organs of infected control mice (Fig. 5*C*). Total and antigen-specific $CD8^+$ T cells, as well as serum viral titres, were all significantly decreased in LCMV-infected $UR^{fl/fl}$;*Lck-Cre* mice throughout the course of the disease (Fig. S7 *B–F*). These results indicate that UVRAG is required for an optimal $CD8^+$ T-cell response to LCMV infection.

Impaired LCMV clearance can result from poor function of effector T cells (24). To investigate if loss of UVRAG hindered not only the expansion of $CD8^+$ T cells but also their differentiation into antigen-specific effector CTLs, we examined the capacity of LCMV-primed effector T cells isolated from LCMV-infected $UR^{fl/fl}$ and $UR^{fl/fl}$;*Lck-Cre* mice to produce IFNγ following ex vivo restimulation. Splenocytes from LCMV-infected mice were stimulated in vitro with GP33 or NP396, and IFNγ production was measured by intracellular cytokine staining plus flow cytometry. The proportion of UVRAG-deficient $CD8^+$ T cells able to produce IFNγ in response to peptide stimulation in vitro was comparable to that in control cultures (Fig. S7*G*), and UVRAG deficiency did not impair the activation of these cells as determined by CD44 up-regulation (Fig. S7*H*, *Left*). Neither were there any significant differences in mutant $CD8^+$ effector T cells in apoptosis (Fig. S7*H*, *Right*), or in cell surface PD-1 (Fig. S7*I*, *Left*) or Fas expression (Fig. S7*I*, *Right*). Therefore, UVRAG is essential for optimal $CD8^+$ T-cell expansion in response to acute LCMV infection, but it does not influence the ability of these residual cells to differentiate into functional effectors.

Lastly, we assessed the role of UVRAG in generating $CD8^+$ memory T cells. The resolution of an acute viral infection is followed by the generation of long-term memory precursor effector cells (MPECs), which express high levels of the IL-7Rα chain (CD127). We compared the kinetics of the appearance and expansion of the MPEC population in $UR^{fl/fl}$ and $UR^{fl/fl}$;*Lck-Cre* mice following acute LCMV infection. As expected, an IL-7Rα^+ $CD8^+$ memory T-cell population arose in control mice by 8 d postinfection, coinciding with the clearance of acute LCMV infection (Fig. 5*D*). However, the appearance of this population was greatly delayed in the absence of UVRAG. Thus, in the context of acute viral infection, UVRAG is required for MPEC generation.

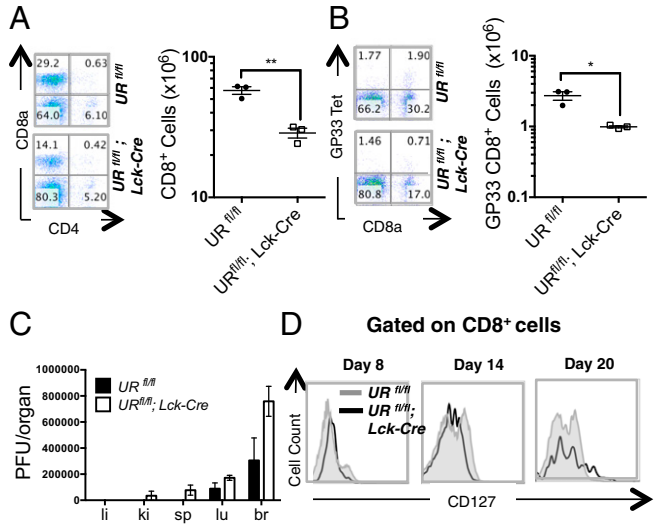

Fig. 5. UVRAG is required for normal responses to acute LCMV infection and MPEC generation. (*A*) Flow cytometric analysis of $CD8^+$ T cells that were isolated from SPL of 6–8 wk old LCMV-infected $UR^{fl/fl}$ and $UR^{fl/fl}$;*Lck-Cre* mice ($n = 3$ per group) and examined on day 8 postinjection. (*Left*) Representative plots of CD4 and CD8 expression. (*Right*) Quantitation of $CD8^+$ T cells in individual mice. Horizontal lines are the cumulative geometric mean ± SEM $^{**}P < 0.005$. (*B*) Flow cytometric analysis of GP33 tetramer-specific $CD8^+$ T cells from the mice in *A*. Data were analyzed as in *A*. $^{*}P < 0.05$. (*C*) Plate count pfu determinations of viral titres in liver (li), kidney (ki), spleen (sp), lung (lu), and brain (br) of the infected mice in *A*. Results are the cumulative mean ± SEM ($n = 3$ per group) and are representative of two independent trials. (*D*) Flow cytometric plot of $CD8^+$ T cells that were $CD127^+$ among PBL isolated on the indicated days postinfection from the infected mice in *A*. Results are representative of one trial involving three mice per group.

Discussion

The objective of this study was to determine the precise roles of UVRAG, known as an autophagic tumor suppressor in many cell types, in T-cell biology. By conditionally deleting the *Uvrag* gene in developing murine T cells in vivo, we have identified an essential and cell-intrinsic role for UVRAG in maintaining the homeostasis of peripheral naïve T cells. Intriguingly, our data suggest that these UVRAG functions are likely independent of its role in autophagy. Indeed, we have shown in vitro that UVRAG is not required for mitophagy and may be a negative regulator of activation-induced autophagy in T cells. In vivo, we have demonstrated that UVRAG is important for T-cell–mediated immune responses to LCMV infection.

Peripheral T-cell homeostasis is a tightly regulated process that ensures the presence of a constant pool of naïve T cells in the secondary lymphoid organs and blood circulation. This pool is maintained by a balance between the influx into the periphery of recent thymic emigrants and the loss of peripheral T cells through normal programmed cell death. Mechanisms that promote the survival and homeostatic proliferation of naïve peripheral T cells are essential for maintaining this balance. Previous work by others has established that IL-7 signaling and interactions between TCRs and self peptide-MHC complexes are crucial for naïve T-cell survival and homeostatic proliferation (25, 26). We have shown here that UVRAG also makes a significant contribution, since naïve T cells lacking UVRAG failed to thrive after adoptive transfer into lymphopenic hosts. However, UVRAG-deficient naïve T cells showed hyperproliferation in response to TCR-mediated stimulation in vitro, implying that the interaction between TCRs and self peptide-MHC complexes on these mutant cells was likely intact. Thus, the exact mechanism underlying UVRAG's role in survival associated with peripheral T-cell homeostasis remains under investigation.

An unexpected finding of our work was that UVRAG was not required for activation-induced autophagy in T cells. In contrast, many in vitro studies have demonstrated that UVRAG is required for both the initiation and maturation of autophagosomes (7–11). Because these activities depend on UVRAG's ability to bind to the Beclin-1 and C/Vps complexes, it was surprising that we did not see a reduction in autophagy in UVRAG-deficient T cells. However, it is possible that UVRAG's role in autophagy is cell type-specific, an issue that will be resolved only by studying UVRAG deletion in other cell types.

In addition to the presence of normal T-cell autophagy, the phenotype of $UR^{fl/fl}$;*Lck-Cre* mice differs significantly from that of other autophagy gene-deficient T-cell–specific mouse models. In contrast to our UVRAG-deficient mutants, mice lacking ATG5, ATG7, ATG3 or Beclin1 in T cells all show peripheral lymphopenia that is largely explained by defects in cell survival and/or impaired

TCR-mediated proliferation (at least in vitro) (1, 3–5). Mice deficient for ATG5 or ATG7 also show impaired clearance of their mitochondria, leading to a build-up of ROS and consequently cell death (1, 4, 5). We found that UVRAG-deficient T cells exhibited not only enhanced autophagy but also normal survival and antigen-induced proliferation in vitro, normal mitochondrial mass, and normal ROS levels. The reasons for these differences with other autophagy-related genes are unknown.

One of our most interesting results was that UVRAG loss had different effects on $CD4^+$ and $CD8^+$ T cells. UVRAG deficiency always led to a greater defect in $CD8^+$ T-cell responses than in $CD4^+$ T-cell responses, both in steady-state mice as well as in BM chimeras. In line with this observation, levels of UVRAG protein were higher in purified $UR^{fl/fl}$ $CD8^+$ T cells compared with $UR^{fl/fl}$ $CD4^+$ T cells. Importantly, this differential effect extended to pathologies involving one or the other of these T-cell subsets. An absence of UVRAG did not increase the susceptibility of mice to EAE induction, a pathology driven by $CD4^+$ Th1 and Th17 cells. However, UVRAG deficiency did render mice more susceptible to infection by LCMV, clearance of which requires effective $CD8^+$ T-cell responses. Further experiments designed to shed light on the differential effect of UVRAG loss on $CD4^+$ and $CD8^+$ T cells are under way.

In conclusion, our data have identified UVRAG as a novel regulator of peripheral T-cell homeostasis, a process crucial for maintaining effective immunity. Furthermore, our findings highlight critical differences between UVRAG and other autophagy-related genes, and indicate that this regulator has important extra-autophagic functions in T-cell biology.

Materials and Methods

Mice. UVRAG floxed ($UR^{fl/fl}$) mice were generated by Cre/LoxP recombination as outlined in Fig. S1*A* using previously described protocols (27). $UR^{fl/fl}$ mice were bred with Lck-Cre transgenic mice (C57BL/6) to generate $UR^{fl/fl}$;*Lck-Cre* mice, which were backcrossed 6 to 10 times to C57BL/6. Mice used in experiments were 4–16 mo old unless otherwise specified. All animal experiments were approved by the University Health Network Animal Care Committee.

Immunoblotting. Extracts of T cells were prepared, fractionated, and transferred to blots as previously described (28), and probed with anti-UVRAG (MBL) or anti-LC3 (MBL) Abs. Loading control Abs were anti–β-tubulin (Sigma-Aldrich) or anti-actin (Sigma-Aldrich). The appropriate Alexa Fluor-conjugated secondary Abs (Molecular Probes) were used to bind to primary Abs and visualized using the Odyssey Infrared Imaging System (LI-COR Biosciences).

Bone Marrow (BM) Chimeras. BM was harvested from femurs and tibias of donor $CD45.1^+$ $UR^{fl/fl}$ or $CD45.2^+$ $UR^{fl/fl}$;*Lck-Cre* mice (≥6 wk old). Total BM cells were subjected to two rounds of $CD4^+/CD8^+$ T-cell depletion using anti-CD4 plus anti-CD8 Abs. Recipient mice (Rag-$2^{-/-}$ or C57BL/6) were irradiated with 6Gy or 10Gy, respectively. $UR^{fl/fl}$ and $UR^{fl/fl}$;*Lck-Cre* BM samples were mixed 1:1, and either $3–5 \times 10^6$ mixed BM cells were transferred i.v. into Rag-$2^{-/-}$ hosts, or $7–10 \times 10^6$ mixed BM cells were i.v. transferred into C57BL/6 hosts. Reconstitution was monitored by analysis of PBL of chimeric mice at 1.5–4 mo postinjection.

T Cell Purification and Activation. Pooled spleen and LN samples were enriched for total T cells using magnetic depletion of other lineages (BD IMag; Miltenyi). Briefly, samples were first incubated with mouse anti-CD16/32 blocking Abs and then with a mixture of biotinylated Abs recognizing Ter119, B220, CD19, CD11b, Nk1.1, and CD11c. For naïve T-cell isolation, biotinylated anti-CD44 Ab was added to the above list. Purified T cells were stimulated with plate-bound anti-mouse CD3 Ab (clone 2C11; BD Biosciences) plus anti-mouse CD28 Ab (clone 37.51; BD Biosciences) at the concentrations indicated in the figures. Where specified, naïve T cells were purified by cell sorting (Facs Aria; Moflow).

Autophagy. For Mitotracker staining, cells were stained for 30 min with 100 nM Mitotracker Green (Invitrogen) in RPMI-1640 complete medium before surface Ab staining and analysis by flow cytometry. For the LC3I-II conversion assay, sorted, naïve T cells were cultured overnight in medium alone, or in plates precoated with 2 μg/mL anti-CD3 Ab plus 0.2 μg/mL anti-CD28 Ab, or anti-CD3/CD28 Abs plus chloroquine (25 μM). Lysates were immunoblotted with Abs recognizing LC3, α-actin, or β-tubulin.

ACKNOWLEDGMENTS. We thank the Princess Margaret Hospital Flow Cytometry facility for cell sorting; Animal Resource Centre for animal care; the CFIBCR PCR Genotyping Facility for genotyping; the Hospital for Sick Children in Toronto for transmission electron microscopy services; Dr. M. E. Saunders for scientific editing of the manuscript; and Dr. Y. Ow, Dr. M. A. Cox, and G. S. Duncan for helpful discussions. This work was supported by grants from the Canadian Institutes of Health Research (to T.W.M. and Z.H.). D.B. is supported by the ATTRACT program of the Luxembourg National Research Fund (FNR). This research was also funded in part by the Ontario Ministry of Health and Long Term Care.

1. Pua HH, Dzhagalov I, Chuck M, Mizushima N, He YW (2007) A critical role for the autophagy gene Atg5 in T cell survival and proliferation. *J Exp Med* 204(1):25–31.
2. Li C, et al. (2006) Autophagy is induced in CD4+ T cells and important for the growth factor-withdrawal cell death. *J Immunol* 177(8):5163–5168.
3. Kovacs JR, et al. (2012) Autophagy promotes T-cell survival through degradation of proteins of the cell death machinery. *Cell Death Differ* 19(1):144–152.
4. Jia W, He YW (2011) Temporal regulation of intracellular organelle homeostasis in T lymphocytes by autophagy. *J Immunol* 186(9):5313–5322.
5. Pua HH, Guo J, Komatsu M, He YW (2009) Autophagy is essential for mitochondrial clearance in mature T lymphocytes. *J Immunol* 182(7):4046–4055.
6. Teitz T, et al. (1990) Isolation by polymerase chain reaction of a cDNA whose product partially complements the ultraviolet sensitivity of xeroderma pigmentosum group C cells. *Gene* 87(2):295–298.
7. Liang C, et al. (2008) Beclin1-binding UVRAG targets the class C Vps complex to coordinate autophagosome maturation and endocytic trafficking. *Nat Cell Biol* 10(7):776–787.
8. Takahashi Y, et al. (2007) Bif-1 interacts with Beclin 1 through UVRAG and regulates autophagy and tumorigenesis. *Nat Cell Biol* 9(10):1142–1151.
9. Liang C, et al. (2006) Autophagic and tumour suppressor activity of a novel Beclin1-binding protein UVRAG. *Nat Cell Biol* 8(7):688–699.
10. Kang R, Zeh HJ, Lotze MT, Tang D (2011) The Beclin 1 network regulates autophagy and apoptosis. *Cell Death Differ* 18(4):571–580.
11. Itakura E, Kishi C, Inoue K, Mizushima N (2008) Beclin 1 forms two distinct phosphatidylinositol 3-kinase complexes with mammalian Atg14 and UVRAG. *Mol Biol Cell* 19(12):5360–5372.
12. Song Z, et al. (2014) Essential role for UVRAG in autophagy and maintenance of cardiac function. *Cardiovasc Res* 101(1):48–56.
13. Lee G, et al. (2011) UVRAG is required for organ rotation by regulating Notch endocytosis in Drosophila. *Dev Biol* 356(2):588–597.
14. Zhao Z, et al. (2012) A dual role for UVRAG in maintaining chromosomal stability independent of autophagy. *Dev Cell* 22(5):1001–1016.
15. Yin X, et al. (2011) UV irradiation resistance-associated gene suppresses apoptosis by interfering with BAX activation. *EMBO Rep* 12(7):727–734.
16. Ge Q, Palliser D, Eisen HN, Chen J (2002) Homeostatic T cell proliferation in a T cell-dendritic cell coculture system. *Proc Natl Acad Sci USA* 99(5):2983–2988.
17. Theofilopoulos AN, Dummer W, Kono DH (2001) T cell homeostasis and systemic autoimmunity. *J Clin Invest* 108(3):335–340.
18. Stephenson LM, et al. (2009) Identification of Atg5-dependent transcriptional changes and increases in mitochondrial mass in Atg5-deficient T lymphocytes. *Autophagy* 5(5):625–635.
19. Hubbard VM, et al. (2010) Macroautophagy regulates energy metabolism during effector T cell activation. *J Immunol* 185(12):7349–7357.
20. Panitch HS, Hirsch RL, Haley AS, Johnson KP (1987) Exacerbations of multiple sclerosis in patients treated with gamma interferon. *Lancet* 1(8538):893–895.
21. Cua DJ, et al. (2003) Interleukin-23 rather than interleukin-12 is the critical cytokine for autoimmune inflammation of the brain. *Nature* 421(6924):744–748.
22. Langrish CL, et al. (2005) IL-23 drives a pathogenic T cell population that induces autoimmune inflammation. *J Exp Med* 201(2):233–240.
23. Hofstetter HH, et al. (2005) Therapeutic efficacy of IL-17 neutralization in murine experimental autoimmune encephalomyelitis. *Cell Immunol* 237(2):123–130.
24. Shin H, et al. (2009) A role for the transcriptional repressor Blimp-1 in CD8(+) T cell exhaustion during chronic viral infection. *Immunity* 31(2):309–320.
25. Sprent J, Cho JH, Boyman O, Surh CD (2008) T cell homeostasis. *Immunol Cell Biol* 86(4):312–319.
26. Khaled AR, Durum SK (2002) Lymphocide: Cytokines and the control of lymphoid homeostasis. *Nat Rev Immunol* 2(11):817–830.
27. Hao Z, Rajewsky K (2001) Homeostasis of peripheral B cells in the absence of B cell influx from the bone marrow. *J Exp Med* 194(8):1151–1164.
28. Hao Z, et al. (2012) The E3 ubiquitin ligase Mule acts through the ATM-p53 axis to maintain B lymphocyte homeostasis. *J Exp Med* 209(1):173–186.